UCRL-JC-126312 Rev.1
PREPRINT

Supernova Hydrodynamics Experiments Using the Nova Laser

B.A. Remington, S.G. Glendinning, K. Estabrook, R.J. Wallace, R. London, R.A. Managan, A. Rubenchik, D. Ryutov, K.S. Budil, J. Kane, D. Arnett, R.P. Drake, R. McCray and E. Liang

This paper was prepared for submittal to the
Supernova 1987A: Ten Years Later
La Serena, Chile
February 22-28, 1997

July 1997

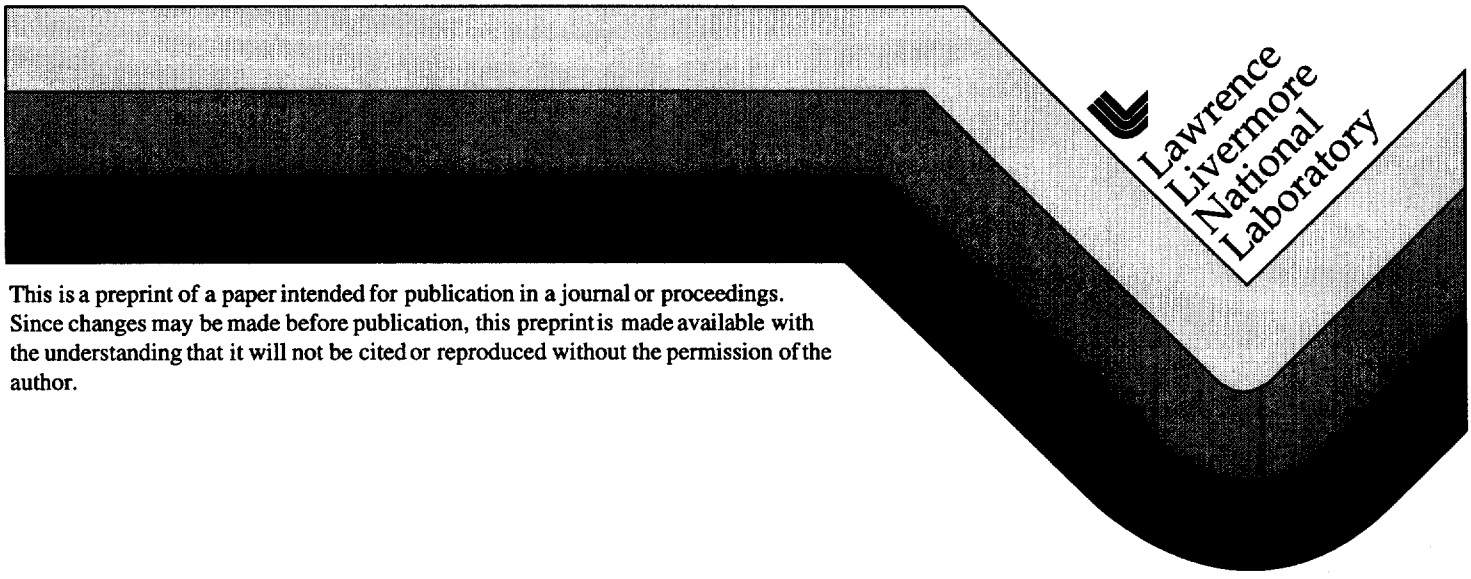

Supernova Hydrodynamics Experiments on Nova

B. A. Remington, S. G. Glendinning, K. Estabrook, R. J. Wallace, R. London, R. A. Managan, A. Rubenchik, D. Ryutov, and K. S. Budil

Lawrence Livermore National Laboratory, P. O. Box 808, Livermore, CA 94550

J. Kane and D. Arnett

Stewart Observatory, University of Arizona, Tucson, AZ 85721

R. P. Drake

University of Michigan, Ann Arbor, MI 48109-2143

R. McCray

University of Colorado-Boulder, JILA, Boulder, CO 80309-0440

E. Liang

Rice University, Houston, Texas 77251

Abstract.

We are developing experiments using the Nova laser to investigate (1) compressible nonlinear hydrodynamic mixing relevant to the first few hours of the supernova (SN) explosion and (2) ejecta-ambient plasma interactions relevant to the early SN remnant phase. The experiments and astrophysical implications are discussed.

Two phases of core-collapse supernova (SN) evolution, the core hydrodynamic mixing in the first few hours and colliding plasmas during early SN remnant formation,(Arnett et al. 1989; McCray 1993) are areas rich with possibilities for supporting laboratory experiments. We report here on two experiments utilizing the Nova laser(Kilkenny 1992) to create the relevant plasma environment.

We start with a progenitor for SN1987A similar to that shown in Fig. 1a from Arnett (1996), and calculate the hydrodynamic evolution using the SN hydrodynamics code PROMETHEUS (Fryxell et al. 1991; Müller et al. 1991). We will focus on the instabilities at the He-H interface. To economize on computing time, we model only $M_r/M_o \geq 5$, depositing the explosion energy, $E = 1.5 \times 10^{51}$ ergs at $M_r/M_o = 5$. This launches a strong radial shock that reaches the He-H interface ($M_r/M_o = 6$) after a transit time of about 100 sec. We show the density and pressure profiles at a time of 4000 sec in Fig. 1b. Note that at the He-H interface ($R \approx 1.0 \times 10^{12}$ cm), the pressure and density gradients are crossed, that is, $\nabla\rho \cdot \nabla P < 0$, such that the He layer is being decelerated by the

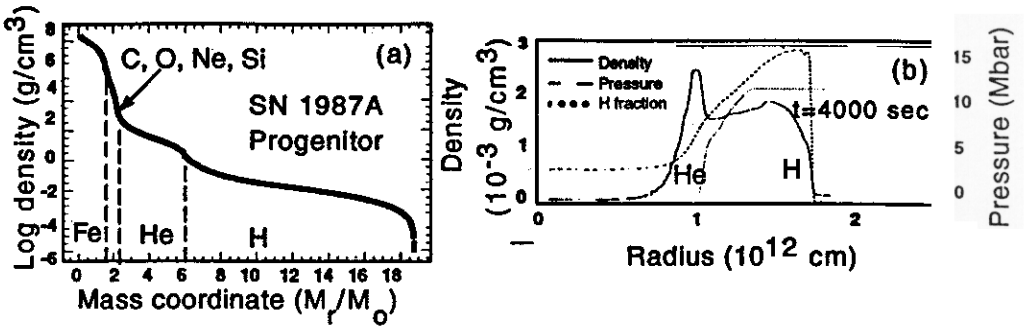

Figure 1. Supernova simulations in 1D of SN1987A.

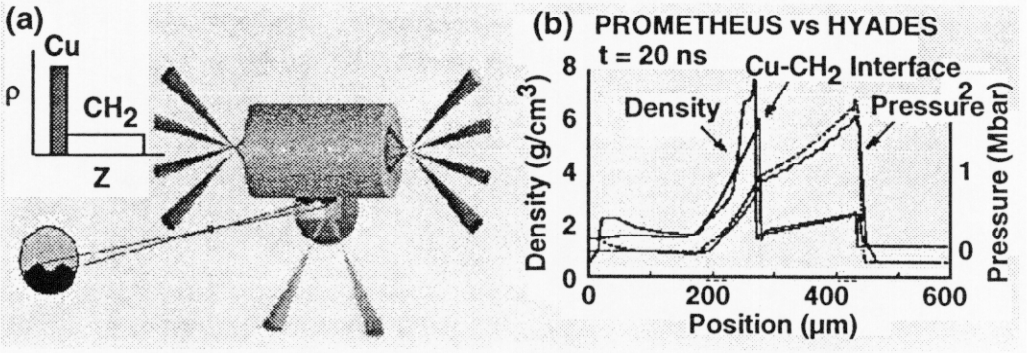

Figure 2. Supernova hydrodynamics experiment.

lower density H layer. This situation is unstable to the Rayleigh-Taylor (RT) instability and perturbations at the interface grow in time. (Fryxell et al. 1991; Müller et al. 1991)

The experimental configuration adopted for these laser experiments is illustrated in Fig. 2a and is described in more depth elsewhere (Remington et al. 1995; Kane et al. 1997; Peyser et al. 1995). Eight of the ten Nova laser beams at a duration of 1 ns and total energy of 12 kJ are focused into a 3.0 mm long, 1.6 mm diameter Au hohlraum (cylindrical radiation cavity) converting to a $\sim$ 190 eV thermal x-ray drive. The experimental package is planar, a 85 μm Cu (ρ =8.9 g/cm^3) foil backed by 500 μm of CH_2 (ρ = 0.95 g/cm^3). A λ = 200 μm wavelength, η_o = 20 μm amplitude sinusoidal ripple is imposed at this embedded interface. The package is mounted across a hole in the hohlraum wall, so that the inner (smooth) side of the Cu sees the x-ray drive. Diagnosis of the interface is through side-on x-ray radiography, using the remaining two Nova beams focused onto an Fe backlighter disk to generate a 5 ns pulse of He-α x-rays at 6.7 keV. In this side-on view, the opaque Cu appears as a shadow, and the CH_2 is essentially transparent.

In Fig. 2b we show the results of modeling in 1D with HYADES,(Larsen & Lane 1994) and PROMETHEUS. (Fryxell et al. 1991; Müller et al. 1991) HYADES is a 1D Lagrangian code with multigroup radiation transport and

tabular equation of state (EOS), and PROMETHEUS is a 3D Eulerian Piecewise Parabolic Method (PPM) code using (here) an ideal gas EOS. We use a measured radiation temperature, $T_r(t)$, as the source input to HYADES, and achieve an impulsive shock acceleration, followed by a protracted deceleration, qualitatively similar to the He-H interface in the SN. We do a high resolution HYADES run, including multigroup radiation transport, for the first 2.45 ns, at which time the shock is approaching the Cu-CH_2 interface. We then map the results to 1D or 2D PROMETHEUS. We compare the results for pressure and density at 20 ns from a continuous 1D HYADES run including radiation transport versus that from PROMETHEUS (Fig. 2b). The mapping works well. Note, the pressures for the Nova experiment, 1-2 Mbar, are not too different from those of the SN (10-15 Mbar), as shown in Fig. 1b, though the SN densities are lower by a factor of about 10^3.

We consider the difference of scales between the SN and the Nova experiment. If we assume that the mixing is dominated by the RT instability, then in the nonlinear regime, the fluid flow can be characterized by a spatial scale of order the perturbation wavelength λ and velocity of order the perturbation terminal bubble velocity $v_B \propto (g\lambda)^{1/2}$. Here g corresponds to the acceleration and we have assumed constant Atwood number. A hydrodynamic time scale is then given by $\tau = \lambda/v_B \propto (\lambda/g)^{1/2}$, and the hydrodynamics equations are invariant under the scale transformation (Hecht et al. 1994; Alon et al. 1995) $\lambda \rightarrow a_1\lambda, g \rightarrow a_2 g$, and $\tau \rightarrow (a_1/a_2)^{1/2}\tau$. We illustrate this transformation, using characteristic scales taken from the simulations shown in Figs. 1 and 2. At 4000 sec for the SN, the deceleration of the He-H interface is $g_{SN} = -1.5 \times 10^4 \mathrm{cm/s^2}$, the density gradient scale length is $L_{SN} = \rho/\nabla\rho = 8\times10^{10}$ cm, and the dominant perturbation wavelength is approximated to be $\lambda_{SN} \approx 10 L_{SN} = 8\times10^{11}$ cm. For the Nova experiment at 20 ns we have $g_{Nova} = -2.5\times10^{13}\mathrm{cm/s^2}$, $\lambda_{Nova} = 2\times10^{-2}$ cm, and a characteristic time interval of $\tau_{Nova} = 5$ ns. The scale transformation is given by $a_1 = \lambda_{SN}/\lambda_{Nova} = 4\times10^{13}$, and $a_2 = g_{SN}/g_{Nova} = 6\times10^{-10}$. The corresponding hydrodynamically equivalent time interval for the SN is then given by $\tau_{SN} = (a_1/a_2)^{1/2}\tau_{Nova} = 1.3 \times 10^3$ sec, which is a reasonable time scale for the SN instability evolution that we are investigating. This scale transformation is not precisely correct, because we have not taken into account the effects of decompression, finite layer thickness, and shocks. Nevertheless, the Nova experiment appears to address the nonlinear compressible hydrodynamics similar to that at the He-H interface of a Type II SN during the first few hours.

In Fig. 3 we show a 2D image from the experiment at 33 ns (Fig. 3a) compared with results from the 2D simulations at 30 ns (Fig. 3b). The experimentally observed perturbation has evolved into the classic nonlinear RT bubble-and-spike shape with peak-to-valley amplitude $\eta_{P/V} \approx 1$, and there are faint indications of Kelvin-Helmholtz roll-ups at the tip of the spike and along its sides. For the simulations, we use the same mapping scheme in 2D as we did in 1D, only now the Cu-CH_2 interface has a $\lambda = 200$ μm wavelength, $\eta_o = 20$ μm amplitude sinusoidal ripple. By 30 ns the perturbation has grown with the opposite phase to an overall peak-to-valley amplitude of $\eta_{P/V} \approx 180\mu\mathrm{m} \approx \lambda$, as shown in Fig. 3b. The shape of the perturbation has changed from sinusoidal to bubble-and-spike, indicating that the interface has evolved well into the nonlinear regime. In Fig. 3c we show the evolution of the spike and bubble

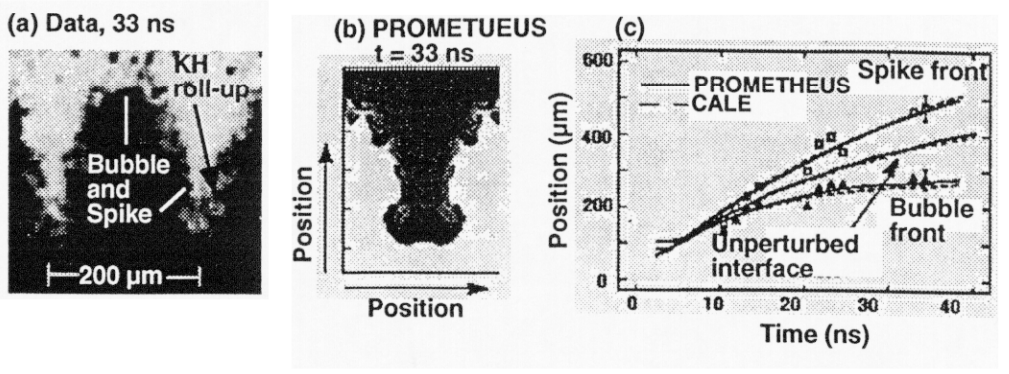

Figure 3. Comparison of data with the simulations.

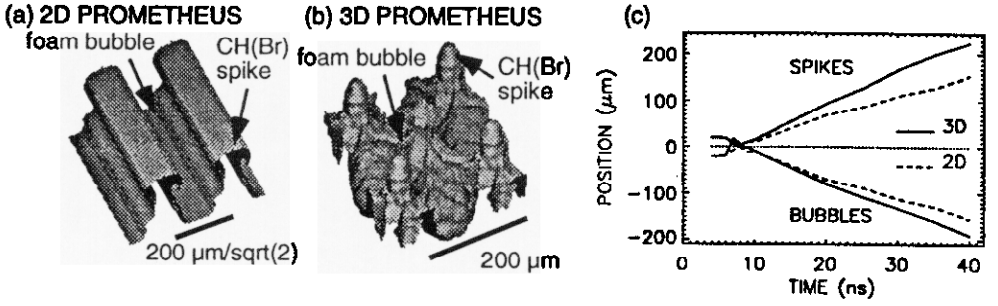

Figure 4. Simulation of RT growth in the nonlinear regime of a 2D versus 3D single mode perturbation. (2D=dotted, 3D=solid).

fronts, compared with the predictions from both PROMETHEUS and CALE, a 2D ALE code (Tipton 1996). The locations of the 2D bubble front and spike front are reproduced very well by both hydrodynamics codes.

We have very recently designed an experiment to illustrate the differences in single-mode RT growth between 2D and 3D, as illustrated in Fig. 4. For target fabrication reasons, the target materials used were changed to CH(Br) for the dense material (ρ = 1.53 g/cm^3) and $CH_{1.1}O_{0.33}$ foam for the lower density material (ρ = 0.07 g/cm^3). These densities were chosen to maintain the same inflight Atwood number ($\sim$ 0.6). The 2D perturbation was a single sinusoid, $\eta = \eta_o \cos(kx)$, with k=$2\pi/\lambda$, and λ = 200 μm/$\sqrt{2}$ = 141 μm and η_o = 20μm. The 3D perturbation corresponded to crossed sinusoids, $\eta = \eta_o \cos(k_x x)\cos(k_y y)$, with $k_{x,y} = 2\pi/\lambda_{x,y}$, where $\lambda_x = \lambda_y$ = 200μm and η_o = 20μm. Results from the simulations in the nonlinear regime (t = 30 ns) for the 2D case are shown in Fig. 4a and for the 3D case in Fig. 4b. The spike and bubble front trajectories are juxtaposed in Fig. 4c, showing that the perturbation spike grows $\sim$ 50% more in 3D. The effect for the bubble is less, but again the bubble grows more in 3D. Similar effects have been observed by a number of other groups doing 3D simulations (Tryggvason & Unverdi 1990; Dahlburg et al. 1993, 1995; Hecht et al. 1995). Experiments will be conducted on the Nova laser in the near future to test this prediction. We are now doing simulations to investigate whether a similar effect occurs in the supernova.

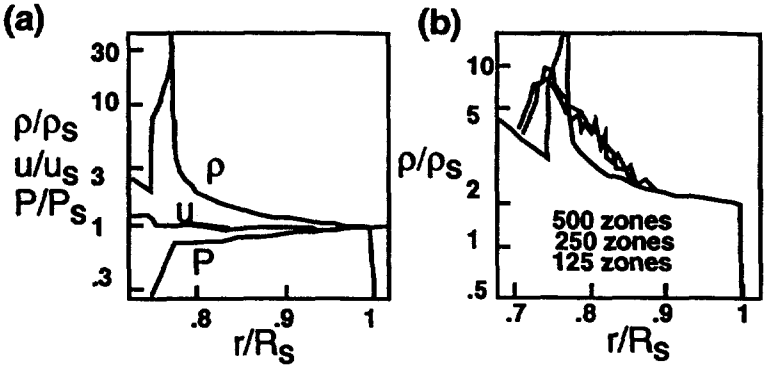

Figure 5. The density, velocity, and pressure profiles for a supernova ejecta-stellar wind interaction. (Reproduced from Chevalier et al. 1992)

Supernovae remnant formation is one of the classic problems of astrophysics. With SN1987A, we have for the first time the opportunity to watch the time-dependent dynamics of the early stages of SN remnant as it evolves. High-velocity supernova ejecta sweep up the surrounding ambient plasma, left over from the stellar wind of the SN progenitor. At the contact discontinuity (the place where the two plasmas meet), shocks are launched forward into the ambient plasma ("forward shock") and backward into the SN ejecta ("reverse shock"), as illustrated with the 1D profiles of density, velocity, and pressure shown in Fig. 5a (from Chevalier et al. 1992). At the contact discontinuity (at $r/R_S = 0.77$ in Fig. 5a), the pressure and density gradients have opposite signs, that is, $\nabla P \cdot \nabla \rho < 0$. Consequently, the shocked circumstellar plasma (of lower density but higher pressure) acts to decelerate the shocked SN ejecta (of higher density but lower pressure). Such a situation is hydrodynamically unstable due to the Rayleigh-Taylor instability, with strong RT growth at the contact discontinuity predicted from 2D simulations (Chevalier et al. 1992; Chevalier & Blondin 1995; Borkowski et al. 1997). This mixing at the contact discontinuity smears out the density profile, as illustrated in Fig. 5b (reproduced from Chevalier et al. 1992). The details of what to expect when the SN1987A ejecta impacts the ring nebula will depend on the structure of both the projectile assembly and the ring. It would be highly beneficial to be able to test these models experimentally prior to the awaited collision.

Hence, our second experiment is focused on testing our understanding of the colliding plasma dynamics in a situation qualitatively similar to that of the ejecta of SN1987A. Our goal is to develop the experiment and model it with the astrophysics codes used to make the predictions of the upcoming ejecta-circumstellar ring collision expected for shortly after the year 2000.

Our initial approach to experimentally simulate the ejecta-wind interaction hydrodynamics is shown in Figure 6a. We use about 20 kJ of laser energy at 0.35 μm laser wavelength, in a 1 ns pulse, to heat a 3 mm long by 1.6 mm diameter cylindrical gold cavity (a hohlraum) to a temperature of about 220 eV. The x-ray flux ablates a CH plug (doped with Br to reduce the transmission of higher-energy x-rays) which is mounted in a 700 μm diameter hole in the

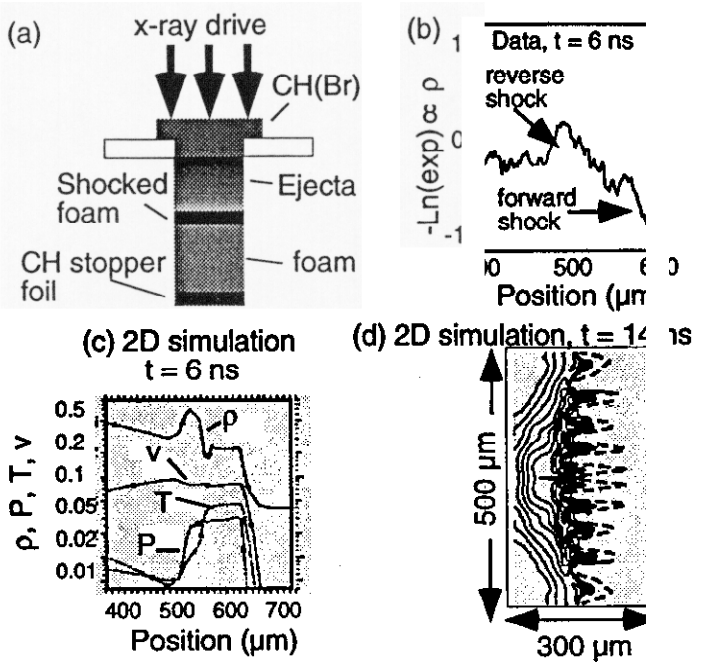

Figure 6. (a) A schematic of the laser experiment. (b) A lineout at 6 ns from the data showing a 1D density profiles at 6 ns. (c) Profiles from the 1D LASNEX simulation at 6 ns showing density (g/cm^3), pressure/100 (Mbar), ion temperature (keV), and velocity ($\times 10^8$ cm/s). (d) Isodensity contours at 14 ns from a 2D LASNEX simulation. The ejecta is flowing into the foam from left to right.

hohlraum. The ablation drives a very strong ($\sim$ 50 Mbar) shock through the CH(Br), ejecting plasma at about 30 eV from the rear of the plug. This plasma (the ejecta) expands and cools. The leading edge of the expansion is a high-Mach-number plasma flow (about Mach 10), although it is at well below solid density. The ejecta impacts a 700 μm diameter cylinder of SiO_2 aerogel foam located 150 μm away and having a density of 40 mg/cm^3. In response, the flowing ejecta stagnates and a shock is driven forward into the foam (forward shock), as well as back into the ejecta (reverse shock).

We diagnose these experiments by x-ray backlighting at 4.3 keV (Sc He_α) to obtain radiographs of the shocked matter. We show a profile of -ln(exposure) $\propto$ density from the data in Fig. 6b and from a LASNEX (Zimmerman & Kruer 1975) simulation in Fig. 6c, both at t = 6 ns. In both the data and simulation, we observe a clear forward shock in the foam, a reverse shock in the ejecta, and a contact discontinuity in between. From the simulations, we see that the shock breaks out of the CH(Br) at about 2 ns, at which time the back edge of the CH(Br) is at a density of about 2 g/cm^3 (compression of $\sim$ 2), pressure of 45 Mbar, and temperature of 30 eV. The foam is impacted by the ejecta about 1 ns later, suggesting that the high velocity tail of the ejecta is moving at $\sim$ 150 μm/ns = 150 km/s. We also show in Figure 6c the pressure, temperature, and velocity of the ejecta-foam assembly from the LASNEX simulation at 6 ns, that

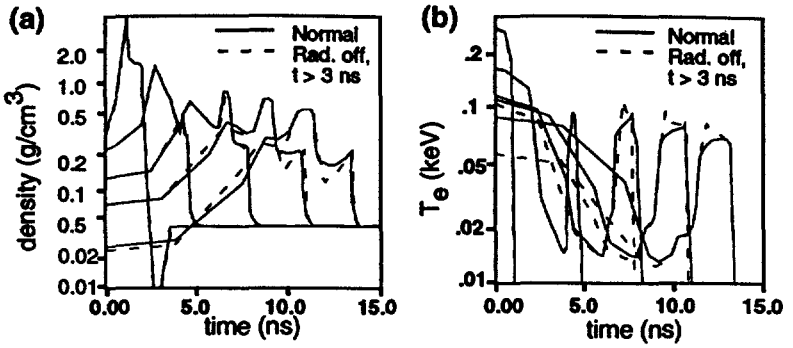

Figure 7. Look-ahead simulations of a similar ejecta-ambient plasma interaction experiment at a higher drive of $T_r = 300$ eV.

is, about 3 ns after the ejecta first starts sweeping up the foam. The contact discontinuity is located at a position of about 560 μm in both the data and the simulation, and the peak densities from the simulation on either side of the contact discontinuity in the ejecta (foam) are 0.65 g/cm^3 (0.25 g/cm^3). The pressure is continuous across the contact discontinuity at a peak value of 3.5 Mbar, the peak temperature is about 50 eV, and the velocity of the projectile assembly is about 1×10^7 cm/sec.

The region near the contact surface at the front of the ejecta is RT unstable (Chevalier et al. 1992; Chevalier & Blondin 1995; Borkowski et al 1997). This is illustrated in Fig. 6d for a 2D simulation of the laser experiment. In the latter, a seed perturbation of wavelength $\lambda = 50$ μm and initial amplitude $\eta_o = 1\mu$m was imposed on the surface of the foam. By 14 ns, strong RT growth of the perturbation well into the nonlinear regime is visible, due to the $\nabla P \cdot \nabla \rho < 0$ configuration at the contact discontinuity (which is indicated by the dashed curve). Comparing Fig. 6d with Fig. 10 from Chevalier et al. (1992), we conclude that both the Nova experiment and the early SN remnant evolution access roughly similar levels of nonlinear RT hydrodynamics. A similar conclusion can be arrived at by comparing linear regime RT growth rates, $\sigma_{\rm linear}$ (e.g. Eq. 6 of Müller et al. 1991), with total duration $\Delta t_{\rm tot}$ of the growth: $1/\sigma_{\rm linear} \ll \Delta t_{\rm tot}$ for both cases. We intend to use this experiment to test the theories and models being used to predict the behavior of SN 1987A, well in advance of the upcoming SN ejecta-ring nebula impact.

As a "look-ahead" exercise, we have done simulations where the drive radiation temperature was increased from 220 eV to $T_r = 300$ eV. Such a drive should be routine on the National Ignition Facility (NIF) laser currently being constructed at LLNL (Paisner et al. 1994; Lindl 1995). Density profiles are shown at 2 ns intervals in Fig. 7a for a nominal simulation (solid) compared to a simulation where radiation is turned off after 3 ns (dashed curve). The corresponding temperature profiles are shown in Fig. 7b. The radiation serves to distribute the heat more evenly behind the forward shock, smoothing out the density valley at the contact discontinuity. The effects of the radiation on the ensuing hydrodynamics will become more prominent at higher drive temperatures, lower target densities, and upon the multiple shock reflections that will occur

when the forward shock impacts a surrogate higher density ring. Experiments where the hydrodynamics depends on correct treatment of radiation transport should be possible on the larger NIF laser currently being built.

In conclusion, we are developing experiments to investigate (1) hydrodynamic instabilities relevant to core collapse supernovae in the first few hours, and (2) ejecta-ambient plasma interaction experiments relevant to the early stages of SN remnant formation. Initial results from both experiments look promising.

References

Alon, U., Hecht, J., Ofer, D., & Shvarts, D. 1995, Phys.Rev.Lett, 74, 534

Arnett, W. D. et al. 1989, ARA&A, 27, 629

Arnett, David 1994, ApJ, 427, 932

Arnett, D. 1996, in Supernovae and Nucleosynthesis, Princeton University Press, Princeton, NJ, 1996

Borkowski, K. J., Blondin, J. M., & McCray, R. 1997, ApJ, 476, L31; 1997, ApJ, in press

Chevalier, R. A., Blondin, J. M., & Emmering, R. T. 1992, ApJ, 392, 118

Chevalier, R. A. & Blondin, J. M. 1995, ApJ, 444, 312

Dahlburg, J. P. et al.1993, Phys. Fluids B, 5, 571; 1995, Phys. Plasmas, 2, 2453

Fryxell, B., Müller, W., & Arnett, D. 1991, ApJ, 367, 619

Hecht, Jacob, Alon, Uri, & Shvarts, Dov 1994, Phys. Fluids, 6, 4019

Hecht, J. et al.. 1995, Laser Part. Beams, 13, 423

Kane, J. et al. 1997, ApJ, in press

Kilkenny, J. D. 1992, Rev. Sci. Instrum., 63, 4688

Larsen, J. T. & Lane, S. M. 1994, J. Quant. Spect. Rad. Trans., 51, 179

Lindl, John 1995, Phys. Plasmas, 2, 3933

McCray R. 1993, ARA&A, 31, 175

Müller, W., Fryxell, B., & Arnett, D. 1991, A&A, 251, 505

Paisner, J. A., Campbell, E. M., & Hogan, W. J. 1994, Fusion Tech., 26, 755

Peyser, T. et al. 1995, Phys.Rev.Lett, 75, 2332

Remington, B. A. et al. 1995, Phys. Plasmas, 2, 241

Tipton, R. 1996, private communication

Tryggvason, G. & Unverdi, S. O. 1990, Phys. Fluids A, 2, 656

Zimmerman, G. B. & Kruer, W. L. 1975, Comments Plasma Phys. Controlled Fusion, 2, 51

Work performed under the auspices of the U.S. Department of Energy by Lawrence Livermore National Laboratory under Contract W-7405-ENG-48.

Technical Information Department • **Lawrence Livermore National Laboratory**
University of California • Livermore, California 94551